



Detection of electronic nematicity using scanning tunneling microscopy

Eduardo H. da Silva Neto,¹ Pegor Aynajian,¹ Ryan E. Baumbach,² Eric D. Bauer,² John Mydosh,³ Shimpei Ono,⁴ and Ali Yazdani^{1,*}

¹*Joseph Henry Laboratories and Department of Physics, Princeton University, Princeton, New Jersey 08544, USA*

²*Los Alamos National Laboratory, Los Alamos, New Mexico 87545, USA*

³*Kamerlingh Onnes Laboratory, Leiden University, 2300 RA Leiden, The Netherlands*

⁴*Central Research Institute of Electric Power Industry, Komae, Tokyo, Japan*

(Received 12 February 2013; revised manuscript received 16 April 2013; published 25 April 2013)

Electronic nematic phases have been proposed to occur in various correlated electron systems and were recently claimed to have been detected in scanning tunneling microscopy (STM) conductance maps of the pseudogap states of the cuprate high-temperature superconductor $\text{Bi}_2\text{Sr}_2\text{CaCu}_2\text{O}_{8+\delta}$ (Bi-2212). We investigate the influence of anisotropic STM tip structures on such measurements and establish, with a model calculation, the presence of a tunneling interference effect within an STM junction that induces energy-dependent symmetry-breaking features in the conductance maps. We experimentally confirm this phenomenon on different correlated electron systems, including measurements in the pseudogap state of Bi-2212, showing that the apparent nematic behavior of the imaged crystal lattice is likely not due to nematic order but is related to how a realistic STM tip probes the band structure of a material. We further establish that this interference effect can be used as a sensitive probe of changes in the momentum structure of the sample's quasiparticles as a function of energy.

DOI: [10.1103/PhysRevB.87.161117](https://doi.org/10.1103/PhysRevB.87.161117)

PACS number(s): 74.72.Kf, 71.27.+a, 74.55.+v, 74.70.Tx

The concept of broken symmetry is essential to condensed matter physics. Identification of the fundamental symmetries of a solid-state system leads to the understanding of the low-energy excitations which govern its properties. For example, the unraveling of the three-decade-old mystery of unconventional superconductivity hinges on determining the symmetries of the correlated electronic state from which Cooper pairs are formed. Recently, electronic nematic phases, where electronic states undergo spontaneous fourfold (C_4) to twofold (C_2) symmetry breaking, have gained much interest as possible candidates for various *hidden order* states in several correlated electron systems such as cuprates, iron-based superconductors, and heavy-fermion materials.^{1–6} However, such states are difficult to detect using nonlocal probes because of possible twin-domain structures in macroscopic samples. Recently scanning tunneling microscopy (STM) has been proposed as the method of choice for the detection of fourfold electronic symmetry breaking.^{7–14} Lawler *et al.*,⁸ and Mesaros *et al.*⁹ in a subsequent study, interpreted the rotational symmetry breaking in the STM data as evidence for an electronic nematic state inside the pseudogap phase of Bi-2212.

The naïve expectation has been that the influence of the STM tip's geometric structure is limited to inducing an easy-to-detect anisotropy in STM topographs or to influence energy-resolved STM differential conductance (dI/dV) maps in an energy-independent manner. Here we show, through model calculations and experimental measurements on three correlated electron materials (CeCoIn₅, Bi-2212, and URu₂Si₂), that a tunneling interference effect within an STM junction composed of a realistic tip (with some spatial anisotropy) can result in an artificial energy-dependent symmetry breaking of the STM conductance maps. This phenomenon can occur even when the STM topograph taken with the same tip appears to be symmetric. We demonstrate that previously reported twofold symmetric conductance maps in high- T_c cuprates^{8,9} are not evidence for rotational symmetry breaking (C_4 to C_2)

originating from a nematic phase in these materials but rather are due to the interference effect we have uncovered here. In this system, systematic measurements with different tips on the same area of the sample, reported here, are also used to clearly demonstrate the lack of nematic order, without relying on any pseudogap-specific assumptions about the tunneling process. We further show that the interference effect within the STM junction can nevertheless be used as a sensitive tool to detect changes in the quasiparticle band structure as a function of energy.

We start our discussion by considering how STM probes the electronic structure of a sample's surface. Following Tersoff and Hamann¹⁵ the sample wave function can be written as

$$\psi_{s,\vec{k}}(\vec{r}) = \sum_{\vec{G}} a_{\vec{G}} \exp[i\vec{k}_G \cdot \vec{r} - (\kappa^2 + |\vec{k}_G|^2)^{\frac{1}{2}} z], \quad (1)$$

where $\vec{k}_G = \vec{k} + \vec{G}$ defines the Wannier states, while $\kappa = \sqrt{2m\phi}/\hbar$ is related to the work function ϕ for electron decay into the vacuum, and the summation is over the reciprocal lattice vectors \vec{G} .¹⁶ Most discussions of STM data assume a metallic tip (energy-independent density of states) and approximate the STM differential conductance dI/dV (at small bias) as the spatial convolution (*) of the tip (ρ_t) and sample (ρ_s) densities of states (DOSs)¹⁵:

$$\frac{dI}{dV}(eV, \vec{r}) \propto \rho_t * \rho_s(eV) \quad (2)$$

with $\rho_s(eV) = \sum_s |\psi_s|^2 \delta(E_s - E_f - eV)$. Then, under the usual assumption of an isotropic tip, the conductance maps are simply proportional to the local DOS of the sample. Within this model of STM measurements the topograph is constructed from integrating such maps between the Fermi level up to the tip-sample bias.

Before considering an anisotropic tip, we emphasize that Eq. (2) above is an approximation of Bardeen's formula for tunneling,^{15–17}

$$I = \frac{e}{\hbar} \sum_{s,t} f(E_s)[1 - f(E_t + eV)] |M_{st}|^2 \delta(\Delta E), \quad (3)$$

where $f(E)$ is the Fermi-Dirac distribution, and $\Delta E = E_s - E_t$. Here M_{st} is the matrix element between the tip and the sample with the following spatial structure¹⁷:

$$M_{st} = \frac{\hbar^2}{2m} \int d\vec{S} \cdot (\psi_s^* \vec{\nabla} \psi_t - \psi_t \vec{\nabla} \psi_s^*). \quad (4)$$

We now demonstrate the effect of the tip geometry on STM measurements, by simulating the conductance maps using Bardeen's matrix element [Eq. (4) above] with a twofold symmetric tip structure, characterized by orthogonal lengths $\delta x = 0.2$, $\delta y = 0.9$ (lattice constant set to unity).¹⁶ We assume that the sample has a C_4 symmetric electronic structure with a generic parabolic band structure [Fig. 1(a)], which is isotropic in the k_x - k_y plane. Calculations of the STM topographic image (at $eV = 3.95t$) and conductance maps at two different energies of this fourfold symmetric sample with elongated-tip wave function are shown in Figs. 1(b)–1(d). While the STM conductance maps can show apparent asymmetry in the x - y plane [Fig. 1(c)], the topograph appears to be remarkably fourfold symmetric [Fig. 1(b)]. Clearly, the summation of dI/dV maps over an appropriate range of energies can lead to a fourfold symmetric topograph. This finding demonstrates that a fourfold symmetric topograph cannot be used as an accurate method to characterize the STM tip geometry, as it is often assumed (for example, see Ref. 8).

An anisotropic tip would naturally induce an apparent breaking of fourfold symmetry in measurements of the electronic structure of a fourfold symmetric sample, as the conductance maps demonstrate. However, the energy dependence of the x - y asymmetry (which can change sign, see below), or its absence for some energies [Fig. 1(d)], points to a previously overlooked interference effect of STM measurements. By examining Eq. (4) we realize that the periodic corrugation along the x and y directions in the conductance maps are determined by the interference [see Fig. 1(h) for schematic] between the sample's quasiparticle states $\psi_{s,\vec{k}}$ with momentum \vec{k} together with those of the tip (characterized in our twofold symmetric tip by δx and δy). Previous studies of the influence of asymmetric tips^{18–20} have overlooked the interference within the STM junction by using the approximation in Eq. (2) which ignores the phase information [$e^{i\vec{k}\cdot\vec{r}}$, see Eq. (1)] of the sample wave functions that are relevant in the evaluation of Eq. (4). Additionally, studies of quantum interference effects in tunneling junctions^{21–24} have not considered the effects of geometrically asymmetric tips on the measurement of long-range periodic structures by the STM. In contrast, our model calculations clearly show that the electronic structure of a fourfold symmetric square lattice probed by a real STM tip can be twofold symmetric depending on the momentum \vec{k} (consequently energy) of the quasiparticles probed.

For a more detailed analysis of the energy-dependence of this asymmetry in STM conductance maps, and to make a connection to experimental measurements, we quantify the

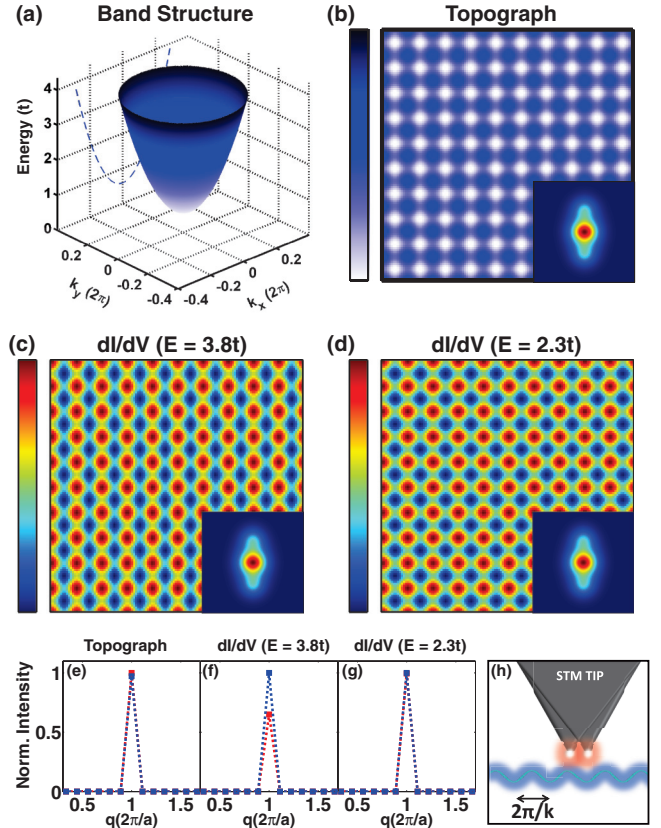


FIG. 1. (Color online) (a) Parabolic band structure [$E = E_0 + tk^2$, with $t = (50/\pi^2)$ and $E_0 = 0.59t$] used to generate panels (b), (c), and (d). (b) Simulated topography at $eV = E = 3.95t$ imaged by the tip in the lower inset. The inset of the tip represents the simulated $|\psi_t|^2$ and is plotted on the same spatial scale as the lattice. (c) Simulated differential conductance at $E = 3.8t$ showing rotational symmetry breaking with the same tip as in panel (b). (d) Simulated differential conductance at $E = 2.3t$ showing no rotational symmetry breaking with the same tip as in panel (b). (e)–(g) Intensities (normalized to the maximum) of the two orthogonal Bragg peaks generated by the DFTs of panels (b)–(d), respectively. (h) One-dimensional schematic representation of the interference between the wave function of a double tip with a quasiparticle state of momentum \vec{k} .

calculated STM conductance maps with the two-dimensional asymmetry parameter that is commonly used in the context of nematic ordering²:

$$O_N(E) = \frac{X(E) - Y(E)}{X(E) + Y(E)}, \quad (5)$$

where $X(E)$ and $Y(E)$ are the energy-dependent amplitudes of the two Bragg peaks along the orthogonal directions obtained from discrete Fourier transformation (DFT), as indicated in Fig. 2(a). A map with $O_N = 0$ corresponds to a fourfold symmetric image, whereas $O_N = 1$ indicates an image with zero corrugation along either the x or y direction (as expected, for example, for one-dimensional stripes). Figure 2(b) shows $O_N(E)$ for different tip configurations. Despite the simplicity of the model band structure, $O_N(E)$ shows a significant energy dependence over the entire bandwidth and even a sign change.

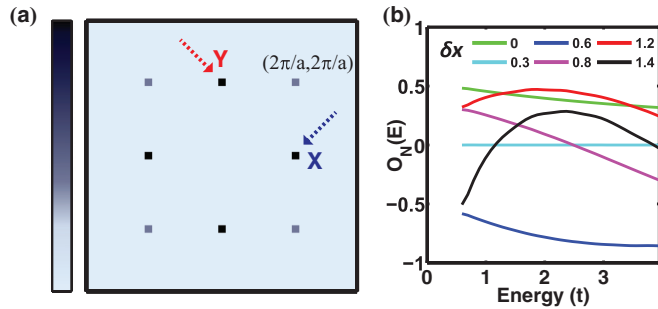


FIG. 2. (Color online) (a) DFT of $dI/dV(E = 0.79t)$ generated using Eq. (2) showing strong peaks due to the long-range periodic lattice structure. (b) Energy dependence of the lattice asymmetry parameter calculated from Eq. (5) for different tip configurations ($\delta y = 0.3$, and δx as indicated in the figure). Notice that for a fourfold symmetric tip [$\delta x = 0.3$ curve in panel (b)] $O_N(E) = 0$ for all energies.

This illustrates the sensitivity of this tip-induced interference effect to the band structure. Although the magnitude of $O_N(E)$ can only be understood by a detailed knowledge of ψ_t , its energy dependence acts as a detector of changes in the momentum structure of the quasiparticle states.

Our model calculation suggests that materials with changes in their electronic band structure as a function of energy (such as a rapid change of band dispersion) are likely to be good candidates for exhibiting the interference effect associated with asymmetric tips. A good material candidate for such a study is the heavy-fermion compound CeCoIn_5 , which crystallizes in the tetragonal crystal structure, ensuring the fourfold symmetry of its electronic states. Recent STM studies on CeCoIn_5 have demonstrated that the electronic structure of this compound exhibits the development of a hybridization gap and associated heavy bands near the Fermi energy at low temperatures.²⁵ Figure 3 shows a topograph [Fig. 3(a)] of CeCoIn_5 , a DFT of a conductance map on the same area [Fig. 3(b)], together with the STM spectrum as a function of energy [Fig. 3(c)], which demonstrates the presence of a hybridization gap in this compound near the Fermi energy. Also shown in Fig. 3 is the intensity of the Bragg peaks in the conductance maps as a function of energy [Fig. 3(d)] and the asymmetry parameter $O_N(E)$ [Fig. 3(e)] introduced above.

Approaching the energy window near the Fermi level, where we expect strong changes in the band structure of CeCoIn_5 due to hybridization of spd - and f -like electrons, we find a strong C_4 -symmetry breaking of the STM conductance maps [Figs. 3(d) and 3(e)]. Both the Bragg peaks and $O_N(E)$ show an energy-dependent asymmetric behavior in tandem with the features of the STM spectrum. The apparent breaking of C_4 symmetry in this experiment is not associated with nematic order in CeCoIn_5 but rather probes the strong momentum dependence of the band structure of this compound near the Fermi level. In fact, it is remarkable that $O_N(E)$ is sensitive to the most subtle features in the spectra as a function of energy [see dashed lines in Fig. 3(c)], which are associated with changes in the electronic momentum structure as previously detected in the quasiparticle interference of this compound.²⁵

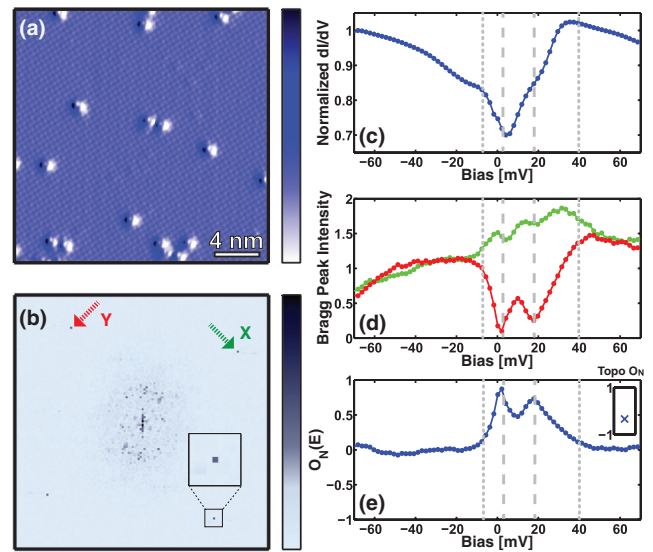


FIG. 3. (Color online) (a) Topograph of CeCoIn_5 (setpoint condition at -200 mV and 1.6 nA) showing a square lattice. For enhanced contrast the derivative of the data is shown. (b) DFT of conductance (dI/dV) map taken at -52 meV over the same field of view (FOV) as panel (a), showing strong Bragg peaks representing the square lattice. Inset shows an enlargement of the bottom right Bragg peak. (c) Tunneling spectrum averaged over the area in panel (a). (d) Energy dependence of the Bragg peak intensity obtained via the DFT operation. (e) Asymmetry parameter calculated via Eq. (5). Inset of panel (e) represents the asymmetry parameter of the topograph acquired simultaneously with the conductance maps.

Further evidence that the asymmetry between X and Y detected in the conductance maps of CeCoIn_5 is associated with interference in the STM junction can be found by repeating the same experiment with slightly different tips (created by interacting with the surface) over the same field of view (FOV) or equivalent areas of the same cleaved sample. As expected from our model calculations [Fig. 2(b)], different tips have different sensitivities to the momentum structure of the electronic structure of the sample and, depending on their geometry, exhibit different degrees of C_4 symmetry breaking in the acquired conductance maps. As Fig. 4(a) shows, the energy dependence of the asymmetry parameter in the conductance maps, $O_N(E)$, is a very strong function of the tip and not always correlated with the presence, or the degree of, Bragg peak asymmetry in the STM topographs of the same area.

We turn our attention next to the claims that STM measurements of underdoped Bi-2212 samples break C_4 symmetry and exhibit nematic order.^{8,9} As shown in Fig. 4(b) measurements on such a sample exhibit characteristics very similar to those of CeCoIn_5 , where changes in the spectrum associated with the pseudogap coincide with apparent asymmetry and a nonzero $O_N(E)$ in this energy window. Not only is this correlation very characteristic of the tip-induced symmetry breaking originating from interference effects within the STM junction, but also we find that $O_N(E)$ displays a strong sensitivity to the tip structure when probing the exact same FOV with slightly different tips. Remarkably, tips that show very similar, nearly x - y symmetric, topographs can show very different energy

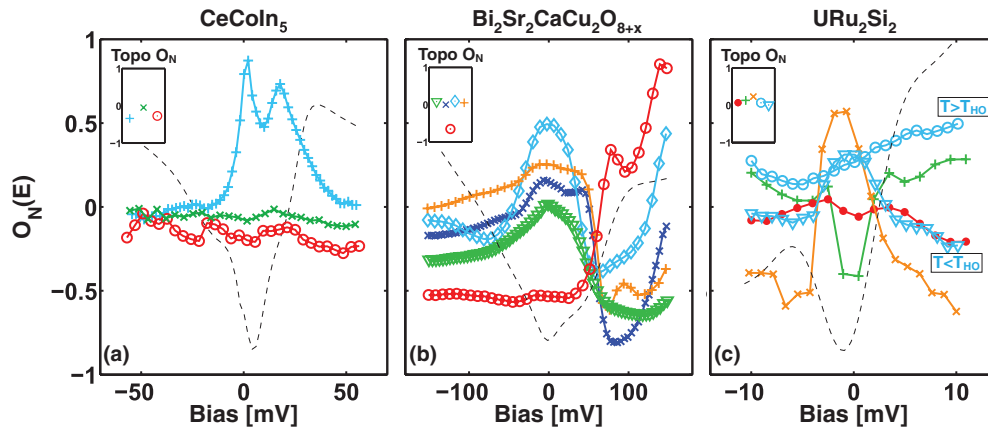


FIG. 4. (Color online) (a) $O_N(E)$ measured on CeCoIn_5 with different tips at 20 K. (b) $O_N(E)$ measured on $\text{Bi}_2\text{Sr}_2(\text{Ca,Dy})\text{Cu}_2\text{O}_{8+\delta}$ ($T_c = 35$ K) at 30 K over the same FOV with different tip configurations. (c) Open symbols represent $O_N(E)$ measured on URu_2Si_2 above T_{HO} (20 K) and below (15 K) over the same FOV with the same tip. Measurements on a second FOV with different tip configurations (closed symbols) were carried out below T_{HO} (15 K). For comparison purposes, the average tunneling spectra are displayed (dashed curves) for the respective materials (for URu_2Si_2 the average spectrum at 10 K is displayed).¹⁶ The insets represent the asymmetry parameter of the respective individual topographs acquired simultaneously to the conductance maps.

dependences for $O_N(E)$ and even exhibit opposite signs for the effect on the same exact area of the sample. Clearly, such behavior is more consistent with the tip-dependent interference in the STM junction, associated with changes in the momenta of electronic states within the pseudogap, rather than any nematic order. Consistent with this view, and with previous experiments,^{8,9} no domain boundaries between regions of different nematic order parameter have ever been found despite the large areas used for STM studies.

Before we conclude, we present experiments on one more materials system, the results of which demonstrate that the interference within the STM junction and the associated asymmetry parameter in fact can be used to probe the onset of sudden changes in electronic band structures of materials. We have carried out temperature-dependent experiments on the heavy fermion URu_2Si_2 , which shows a sharp second-order phase transition in the so-called hidden order state below $T_{HO} = 17.5$ K, the nature of which continues to be a mystery.^{26–28} Experiments on this compound are also consistent with the asymmetry parameter picking up changes in the electronic states at low temperatures through the tip-dependent interference. However, contrasting measurements below and above the T_{HO} , over the same FOV, and with the same tip [open symbols in Fig. 4(c)], show that the signals in $O_N(E)$ change from a peaklike shape to a smooth curve, directly reflecting the change in the band structure as the hidden-order phase transition is crossed. At temperatures just below the transition, when the changes in the electronic states are difficult to detect in the STM spectra, we find that $O_N(E)$ is extremely sensitive to the changes that occur in the electronic structure of this material below T_{HO} .

Overall, our systematic measurements on three different materials (with three different characteristic gap energy scales, 30 meV for CeCoIn_5 , 4 meV for URu_2Si_2 , and 100 meV for Bi-2212), demonstrate the strong sensitivity of the asymmetry parameter $O_N(E)$ to different tip configurations and,

specifically, how it can change sign for measurements over the same FOV. From these results, we can only conclude that $O_N(E)$ is not a measure of the symmetry breaking of the electronic states of the sample; rather it is the result of the interference effect which is evident in the elementary model of tunneling from a realistic tip discussed in here. Although STM can in principle detect the onset of nematic order, we have demonstrated that symmetry analyses of conductance maps can be dominated by the energy dependence of the band structure of the sample rather than nematic order. Perhaps the only experimentally reliable approach to detect rotational symmetry-breaking order with the STM would be to image the presence of domain boundaries, such as the structural ordering¹⁰ and electronic smectic ordering⁹ in Bi-2212 , and electronic nematic ordering in iron-based superconductors.^{7,14} Alternatively rotation of the STM tip by an appropriate angle (90° in the case of C_4 symmetry) while maintaining the same location on the sample could be developed to discount the role of the tip geometry. Regardless, the interference within the STM junction with realistically anisotropic tips described here shows that such measurements are a sensitive probe of the changes in the quasiparticle states of the sample as a function of energy, even when such changes might not be apparent in STM spectra.

Work at Princeton University was primarily supported by a grant from the DOE Office of Basic Energy Sciences (DE-FG02-07ER46419). The instrumentation and infrastructure at the Princeton Nanoscale Microscopy Laboratory are also supported by grants from the NSF-DMR1104612 and NSF-MRSEC programs through the Princeton Center for Complex Materials (DMR-0819860). Work at LANL was conducted under the auspices of the US DOE Office of Basic Energy Sciences, Division of Materials Science and Engineering.

*yazdani@princeton.edu

- ¹S. A. Kivelson, I. P. Bindloss, E. Fradkin, V. Oganesyan, J. M. Tranquada, A. Kapitulnik, and C. Howald, *Rev. Mod. Phys.* **75**, 1201 (2003).
- ²E. Fradkin, S. A. Kivelson, M. J. Lawler, J. P. Eisenstein, and A. P. Mackenzie, *Ann. Rev. Cond. Matt. Phys.* **1**, 153 (2010).
- ³R. Daou, J. Chang, D. LeBoeuf, O. Cyr-Choiniere, F. Laliberte, N. Doiron-Leyraud, B. J. Ramshaw, R. Liang, D. A. Bonn, W. N. Hardy, and L. Taillefer, *Nature (London)* **463**, 519 (2010).
- ⁴J.-H. Chu, J. G. Analytis, K. De Greve, P. L. McMahon, Z. Islam, Y. Yamamoto, and I. R. Fisher, *Science* **329**, 824 (2010).
- ⁵R. Okazaki, T. Shibauchi, H. J. Shi, Y. Haga, T. D. Matsuda, E. Yamamoto, Y. Onuki, H. Ikeda, and Y. Matsuda, *Science* **331**, 439 (2011).
- ⁶J.-H. Chu, H.-H. Kuo, J. G. Analytis, and I. R. Fisher, *Science* **337**, 710 (2012).
- ⁷T.-M. Chuang, M. P. Allan, J. Lee, Y. Xie, N. Ni, S. L. Budko, G. S. Boebinger, P. C. Canfield, and J. C. Davis, *Science* **327**, 181 (2010).
- ⁸M. J. Lawler, K. Fujita, J. Lee, A. R. Schmidt, Y. Kohsaka, C. K. Kim, H. Eisaki, S. Uchida, J. C. Davis, J. P. Sethna, and E. Kim, *Nature (London)* **466**, 347 (2010).
- ⁹A. Mesaros, K. Fujita, H. Eisaki, S. Uchida, J. C. Davis, S. Sachdev, J. Zaanen, M. J. Lawler, and E.-A. Kim, *Science* **333**, 426 (2011).
- ¹⁰I. Zeljkovic, E. J. Main, T. L. Williams, M. C. Boyer, K. Chatterjee, W. D. Wise, Y. Yin, M. Zech, A. Pivonka, T. Kondo, T. Takeuchi, H. Ikuta, J. Wen, Z. Xu, G. D. Gu, E. W. Hudson, and J. E. Hoffman, *Nat. Mater.* **11**, 585 (2012).
- ¹¹M. H. Hamidian, I. A. Firmo, K. Fujita, S. Mukhopadhyay, J. W. Orenstein, H. Eisaki, S. Uchida, M. J. Lawler, E.-A. Kim, and J. C. Davis, *New J. Phys.* **14**, 053017 (2012).
- ¹²C.-L. Song, Y.-L. Wang, P. Cheng, Y.-P. Jiang, W. Li, T. Zhang, Z. Li, K. He, L. Wang, J.-F. Jia, H.-H. Hung, C. Wu, X. Ma, X. Chen, and Q.-K. Xue, *Science* **332**, 1410 (2011).
- ¹³Y. Kohsaka, T. Hanaguri, M. Azuma, M. Takano, J. C. Davis, and H. Takagi, *Nat. Phys.* **8**, 534 (2012).
- ¹⁴C.-L. Song, Y.-L. Wang, Y.-P. Jiang, L. Wang, K. He, X. Chen, J. E. Hoffman, X.-C. Ma, and Q.-K. Xue, *Phys. Rev. Lett.* **109**, 137004 (2012).
- ¹⁵J. Tersoff and D. R. Hamann, *Phys. Rev. B* **31**, 805 (1985).
- ¹⁶See Supplemental Material at <http://link.aps.org/supplemental/10.1103/PhysRevB.87.161117>.
- ¹⁷J. Bardeen, *Phys. Rev. Lett.* **6**, 57 (1961).
- ¹⁸D. Tománek, S. G. Louie, H. J. Mamin, D. W. Abraham, R. E. Thomson, E. Ganz, and J. Clarke, *Phys. Rev. B* **35**, 7790 (1987).
- ¹⁹E. J. Snyder, E. A. Eklund, and R. Williams, *Surf. Sci.* **239**, L487 (1990).
- ²⁰W. Sacks, D. Roditchev, and J. Klein, *Phys. Rev. B* **57**, 13118 (1998).
- ²¹L. Jureczyszyn, A. Rosenhahn, J. Schneider, C. Becker, and K. Wandelt, *Phys. Rev. B* **68**, 115425 (2003).
- ²²L. Jureczyszyn and B. Stankiewicz, *Prog. Surf. Sci.* **74**, 185 (2003).
- ²³J. A. Nieminen, E. Niemi, and K.-H. Rieder, *Surf. Sci.* **552**, L47 (2004).
- ²⁴N. V. Khotkevych, Y. A. Kolesnichenko, and J. M. van Ruitenbeek, *Low Temp. Phys.* **37**, 53 (2011).
- ²⁵P. Aynajian, E. H. da Silva Neto, A. Gyenis, R. E. Baumbach, J. D. Thompson, Z. Fisk, E. D. Bauer, and A. Yazdani, *Nature (London)* **486**, 201 (2012).
- ²⁶T. T. M. Palstra, A. A. Menovsky, J. v. d. Berg, A. J. Dirkmaat, P. H. Kes, G. J. Nieuwenhuys, and J. A. Mydosh, *Phys. Rev. Lett.* **55**, 2727 (1985).
- ²⁷P. Aynajian, E. H. da Silva Neto, C. V. Parker, Y. Huang, A. Pasupathy, J. Mydosh, and A. Yazdani, *Proc. Natl. Acad. Sci. USA* **107**, 10383 (2010).
- ²⁸A. R. Schmidt, M. H. Hamidian, P. Wahl, F. Meier, A. V. Balatsky, J. D. Garrett, T. J. Williams, G. M. Luke, and J. C. Davis, *Nature (London)* **465**, 570 (2010).